Epidemics 2 (2010) 195–206

Contents lists available at ScienceDirect

Epidemics

journal homepage: www.elsevier.com/locate/epidemics

Epidemics and control strategies for diseases of farmed salmonids: A parameter study

A.R.T. Jonkers [a,b], K.J. Sharkey [c,*], M.A. Thrush [d], J.F. Turnbull [e], K.L. Morgan [f]

[a] Institute for Geophysics, University of Münster, Corrensstrasse 24, Münster 48149, Germany
[b] Department of Earth & Ocean Sciences, University of Liverpool, 4 Brownlow Street, Liverpool, L69 3GP, UK
[c] Department of Mathematical Sciences, University of Liverpool, Liverpool, L69 7ZL, UK
[d] Centre for Environment Fisheries and Aquaculture Science (Cefas), Barrack Road, Weymouth, DT4 8UB, UK
[e] Institute of Aquaculture, University of Stirling, Stirling, Stirlingshire, FK9 4LA, UK
[f] Department of Veterinary Clinical Science, University of Liverpool, Leahurst, Neston, CH64 7TE, UK

ARTICLE INFO

Article history:
Received 19 May 2010
Revised 2 August 2010
Accepted 24 August 2010

Keywords:
Epidemiology
Simulation
Contact networks
Control policies
Balanced ANOVA

ABSTRACT

The susceptibility of the English and Welsh fish farming and fisheries industry to emergent diseases is assessed using a stochastic simulation model. The model dynamics operate on a network comprising directed transport and river contacts, as well as undirected local and fomite transmissions. The directed connections cause outward transmission risk to be geographically more confined than inward risk. We consider reactive, proactive, and hybrid methods of control which correspond to a mixture of policy and the ease of disease detection. An explicit investigation of the impact of laboratory capacity is made. General quantified guidelines are derived to mitigate future epidemics.

Introduction

Aquatic ecosystems have inherent biological and ecological value. In addition, humans rely on them for profit, recreation, livelihood, and nutrition (Food and Agriculture Organisation of the United Nations, 2004). Aquatic animals are an important component of these systems and they suffer from many infectious diseases, associated with a broad range of pathogens (viral, bacterial, fungal, protozoal, and metazoal) many of which have the potential to cause disease epidemics. Viral pathogens affecting northwest European fish stocks include several distinct strains of Salmonid Alpha Viruses (SAV, responsible for pancreas disease and sleeping disease), Infectious Pancreatic Necrosis virus (IPNV), Viral Haemorrhagic Septicaemia virus (VHSV, identified in at least 48 different marine and freshwater species), and Infectious Haematopoietic Necrosis virus (IHNV) (LaPatra et al., 2001; Skall et al., 2005; McLoughlin and Graham, 2007; Rodger and Mitchell, 2007; Stone et al., 2008; Munro et al., 2010). In England and Wales, some bacterial diseases affecting in particular salmonids (*Salmonidae*), include Bacterial Kidney Disease (BKD, *Renibacterium salmoninarum*), *Lactococcus garvieae* (LG, identified in England in 2000), and Enteric Redmouth disease (ERM, *Yersinia ruckeri*) (Tobback et al., 2007; Chambers et al., 2008; Algöet et al., 2009). An important parasitical threat is *Gyrodactylus salaris* (GS, Peeler and Thrush, 2004).

The effects of these pathogens can be devastating to fish stocks. For example, observed mortality levels of sleeping disease in France reached 22% in the 1990s, whereas pancreas disease in Ireland in 1989–1994 resulted in up to 48% mortality in 43 separate outbreaks (McLoughlin and Graham, 2007; Rodger and Mitchell, 2007). VHSV-associated mortality in rainbow trout (*Oncorhynchus mykiss* (Walbaum)) can be up to 100% in fry, and 30–70% in older fish (Skall et al., 2005). Similarly high proportions have been reported for IHNV, with up to 100% mortality in salmonid fry (Hattenberger Baudouy et al., 1995). Detrimental subclinical effects may include lethargy and loss of appetite (Damsgård et al., 1998; Rodger and Mitchell, 2007; Algöet et al., 2009).

Pathogen-induced fish mortality and suppressed growth also have severe socio-economic consequences (e.g. Lilley and Roberts, 1997; Food and Agriculture Organisation of the United Nations and Network of Aquaculture Centres in Asia, 2001). For instance, it was estimated in 1998 that VHSV caused the western European aquaculture industry circa US$ 60 million per year (Giorgetti, 1998), whereas Iversen et al. (2005) assessed the direct costs of disease for Norwegian fish farming around US$ 150 million annually. Clearly, much is to be gained from a better understanding of how these diseases spread, which sites, regions, or river catchments are most at risk, which parameters are most influential, and which mitigation strategies might be most effective in outbreak control. Here we present our efforts to statistically quantify these aspects by means of a large-scale

* Corresponding author. Fax: +44 151 794 4754.
E-mail address: kjs@liv.ac.uk (K.J. Sharkey).

1755-4365/$ – see front matter © 2010 Elsevier B.V. All rights reserved.
doi:10.1016/j.epidem.2010.08.001

epidemiological simulation, based on the actual network configuration of 2090 English and Welsh fish farms and fisheries that stock and rear salmonids.

Materials and methods

Network nodes and connections

The epidemiological significance of simulated contact networks is well established (e.g., Kiss et al., 2005, 2006a,b; Sharkey et al., 2008). Unlike mean-field approximations, each network node or site is considered unique, with specific coordinates (here: U.K. Ordnance Survey grid), specific connected or unconnected neighbouring nodes, and specific transmission paths or links whose associated likelihood differs per type (Kiss et al., 2006b; Sharkey, 2008). This allows for a more realistic representation of contacts, including spatial heterogeneity in the number of links (e.g., scale-free networks), distinction between directed and undirected links, the effects of long-range connections (e.g., small-world networks), and emergent properties due to clustering, community association, or fragmentation of network parts (Keeling, 1999; Sharkey et al., 2006; Green et al., 2009; Munro and Gregory, 2009; Jonkers et al., 2010).

The English and Welsh network studied here comprises 2090 distinct sites, comprising 235 fish farm and 1855 fishery sites, distributed among 155 river catchments of very wide size range (Fig. 1). Four catchments (Thames, Severn, Trent, and the Yorkshire Ouse) contain over one hundred sites each; another 46 catchments have between 10 and 100 sites, 75 more each hold 2–9 sites, and the remaining 30 contain a single site. These totals demonstrate some of this network's spatial heterogeneity. Moreover, complexity increases markedly once the connections between these nodes are taken into account. For the purpose of our simulations we distinguish four distinct transmission mechanisms depicted in Fig. 2: directed transport (live fish movement) and directed river transmissions, and undirected local and fomite transmissions.

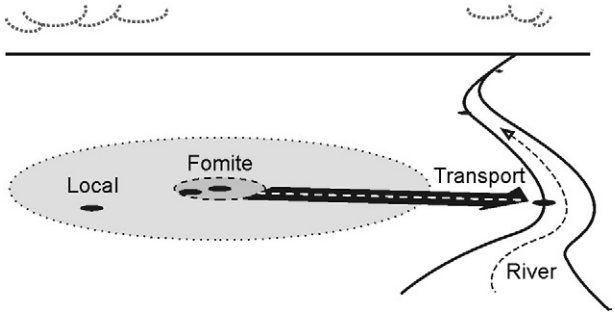

Fig. 2. The four types of transmission considered: the likelihood of local and fomite connections (undirected) decreases with geographical distance (circles with radius 25 and 5 km respectively) from a source site (small black circle). Transport and (downstream) river links are directed contacts of unlimited range.

The analysed contact structure has a number of remarkable features, notably, it is not a scale-free network. Histograms of the number of links per site (see Supplement) show that almost all sites are highly connected. This is primarily due to the tens of thousands of short-range, bidirectional connections between nearby sites. Although their transmission likelihood is low and decreases sharply with distance, their sheer number creates a dense mesh of localised links, theoretically allowing a pathogen to roam from one end of the network to another in a long sequence of small steps. Superimposed on this foundation is the transport system, which reliably and quickly distributes live hosts and pathogens from less than two hundred (fish farm) sources to over two thousand destinations (98.3% of the network). Fisheries thus function purely as receivers of transport transmissions, creating a profound asymmetry. A second series of more geographically confined conduits is provided by the rivers on which many fish farms and fisheries are

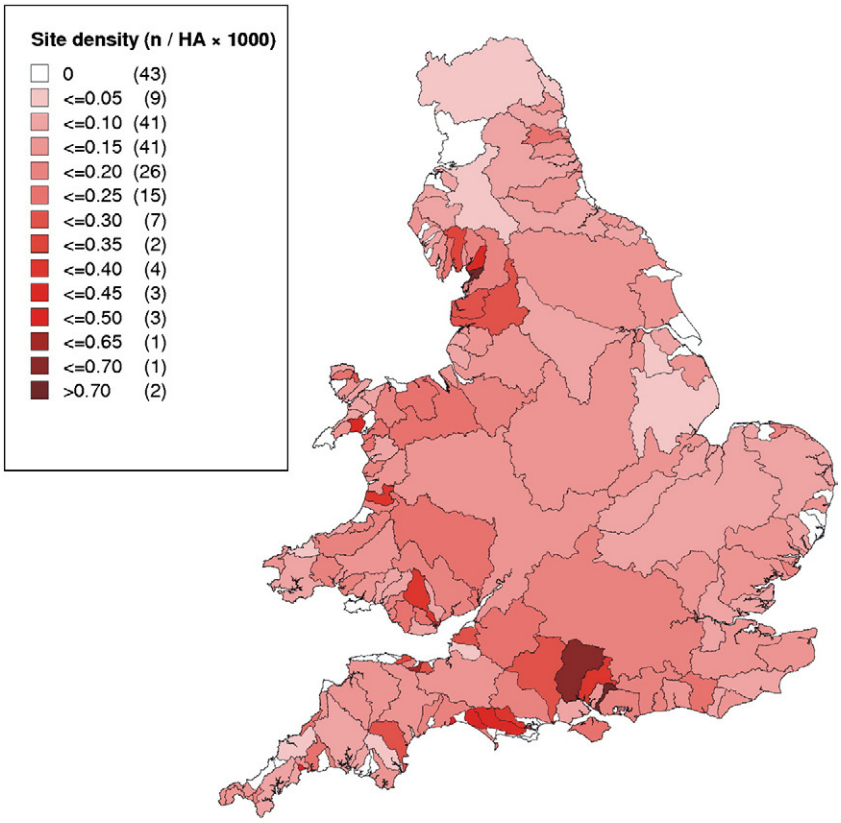

Fig. 1. Site density per river catchment in England and Wales in 2004 (number of sites per thousand hectares of the catchment area).

situated. The majority of these transport and river links span great distances, resulting in a network that can be classified as of the "small-world" type (Moore and Newman, 2000). Thus the (relatively high-likelihood) bridging paths between distant local clusters cause the shortest route between any two sites to require few intermediary steps on average.

Transport transmission

Transport by road haulage involves the movement of live, pathogen-carrying fish (including potentially pathogen-carrying water or equipment) between two sites (Murray, 2006; Gustafson et al., 2007). It involves transfer of fingerlings from hatcheries to on-growing sites, stocking of fisheries, and occasionally the movement of fish to processing plants (Murray and Peeler, 2005; Munro and Gregory, 2009). This type of (often long-distance) transmission is highly dangerous, as the empirical record attests: Skall et al. (2005) identified transports of infected farmed fish as the primary means of spread and major cause of VHSV in Europe; Green et al. (2009) noted the implication of road transports of live rainbow trout in the U.K.-wide spread of BKD in 2005. Murray et al. (2002) highlighted the role of live transports (in well boats) in the 1998 outbreak of Infectious Salmon Anaemia (ISA) in Scotland, and Peeler and Thrush (2004) identified empty fish transporters returning from infected areas as the highest risk regarding the introduction of GS from mainland Europe into Britain.

Under EU directive 2006/88/EC, EU member states are now required to perform risk-based surveillance of aquatic diseases, and to record live fish movements (Green et al., 2009; Munro and Gregory, 2009). Fish farmers therefore have a legal obligation to keep records of all movements of live fish on and off their sites and to make this information available to the competent authority for the control of notifiable fish diseases; for England and Wales this is the Centre for Environment, Fisheries and Aquaculture Science (Cefas). Movements to recreational fisheries or open waters for restocking furthermore require consent from the Environment Agency (EA) under Section 30 of the Salmon and Freshwater Fisheries Act (Anonymous, 1975). Cefas maintains these records on the Live Fish Movement Database (LFMD). The LFMD was interrogated to determine all destinations of live fish movements made in 2004 from each fish farm that was registered on the database in September 2006 for holding stocks of salmonid fish (rainbow trout *O. mykiss*, brown trout *Salmo trutta* and Atlantic salmon *Salmo salar*) and a contact network was constructed on the basis of this trading activity.

The epidemiological risk of site-to-site transports of live animals can be explored quantitatively through network analysis, as reported for a number of other farmed species such as cattle, sheep, and pigs (e.g., Christley et al., 2005; Webb, 2005; Bigras-Poulin et al., 2007). Within the U.K., Munro and Gregory (2009) have identified sites that are vulnerable and have a high-risk of spreading infections in the network architecture of Scottish farmed salmonid movements in 2004, whereas Thrush and Peeler (2006) developed a stochastic simulation model to study pathogen spread involving site-to-site movement. In the present study, we used a total of 4530 recorded transports along 2750 routes, departing from 194 distinct sites and servicing almost the entire network (2055 sites). Given a maximum time span of thirty years per simulated outbreak, seasonal fluctuations were ignored when computing the likelihood per day of transport transmission, based on the number of annual transports T per site:

$$p_{trans} = T / 365.2524.$$

Transports from an infected site are considered to cease immediately upon notification of that site.

River transmission

The second transmission type considered was river transport (2232 links), comprising several distinct mechanisms. Infected fish may release pathogens via urine and reproductive fluids, etc. These pathogens may then be swept along by river flow or wild fish may act as carriers (Skall et al., 2005; Peeler et al., 2008; Taylor et al., 2010). Additional factors include pleasure boat traffic, angling equipment, wind and solar effects, the presence of chemical pollutants, suspended solids, or interaction between organisms (Toranzo and Hetrick, 1982; Murray et al., 2005). These effects are difficult to quantify (see Discussion). Consequently, our simulations disregard most of these, concentrating on an empirically-founded, stochastic representation of downstream particle flow only, as pathogen spreading through infected water or suspended particles is considered more likely in a downstream direction (McAllister and Bebak, 1997; Sharkey et al., 2006).

We implemented an algorithm that takes into account the distance along a river between two sites (generally larger than the Euclidean distance), the asymmetry of the contact network (using downstream links), and stochastic sampling of an empirically derived distribution of river stream flow speeds. The river contact network was compiled using a customised adaptation of the Intelligent River Network developed by the Centre for Ecology and Hydrology (CEH) to generate inter-site distances through the river network for farm and fishery locations provided by Cefas. Estimation of river flow speeds initially proved problematic, as publicly available data on river resources maintained by the U.K. Environment Agency are stored as different flow parameters such as cumecs (cubic meters of water per second), which cannot be converted into flow speeds without detailed knowledge of depth and shape of the local riverbed at each sampling point.

Instead we trawled the United States Geological Survey's water resources (at http://waterdata.usgs.gov/usa/nwis, section surface water, daily data) for some 350 river sites with daily means of stream flow speeds. Of these, 37 locations provided over one hundred consecutive sampled days each (capped per site at three years of data, to avoid bias due to a few anomalously long records), yielding over 25 thousand positive daily means in total. A plot of their binned frequencies (Fig. 3) reveals a loglinear distribution ranging from 0.05 to 4.4 m/s, with lowest speeds being most prevalent. Sampling from such a global distribution disregards localised effects of gradient, depth, and surface area. However, given the gathered flow speeds, a large part of this variability is assumed to be captured in the broad observed range, which spans almost an order of magnitude. Other than the incorporated measured distances between sites along a river trajectory, we have made no attempt to represent seasonality or

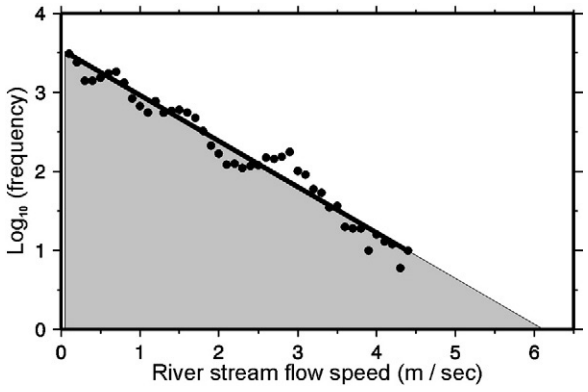

Fig. 3. River stream flow speed distribution and loglinear best fit; percentage of variation explained by the fit: 96.2%. Original sample: 25,088 daily means from 37 U.S. locations measured by USGS, binned per 0.1 m/s ($N = 44$). The shaded (loglinear) area is repeatedly sampled to determine riverborne transit times.

different river types (e.g., meandering, braided, delta, white-, black-, or clearwater, etc.).

We subsequently determined for each river connection how long a waterborne particle might take on average from source to destination. We computed total transit time by repeatedly updating the cumulative distance travelled, based on a flow speed drawn randomly from the distribution for each 24 h spent in the water, until the destination was reached. Thus the simulated flow speeds within the same river would be different for each connection (being itself a cumulative composite of sampled daily average velocities). Despite some English and Welsh river distances exceeding 100 km (average: 17.1 km), most site-to-site river intervals computed with this method take less than two days (max: 5 days). This suggests that if the sampled rivers can be deemed comparable to U.K. rivers in their flow speeds, most fish pathogens should be considered well able to survive these (and longer) journeys. In this context, McAllister and Bebak's (1997) report of detecting significant IPNV titre levels almost 20 km downstream from an infected source site is not unexpected.

The outbreak simulator applied the described repeated stochastic sampling to compute θ, the total time (in days and parts thereof) the pathogen spent in transit. We furthermore assume that the likelihood of transmission decays exponentially over time by dilution and entrapment in substrate or vegetation. Note that this dilution effect is independent of pathogen viability. Given an average daily transmission rate α, we define river transmission likelihood here as:

$$p_{river} = \alpha \exp\left[-\theta\lambda_R\right].$$

The final scalar λ_R in this equation is set to unity, which represents a waterborne pathogen decay rate of $1/e \approx 0.37$ per day, implying a 3-$\log_{10}$ reduction in virus titre ($T_{99.9}$) after 7 days. Laboratory studies report a wide range of such inactivation rates, depending on pathogen, water temperature, salinity, and the presence of additional substances. Given freshwater at 20 °C, Toranzo and Hetrick (1982) and Barja et al. (1983) estimate a 9-day inactivation rate of IPNV versus 14 days for IHN, whereas Murray et al. (2005) adopt an hourly decay rate of 10% for ISA (i.e., inactivation after 3 days), and Kocan et al. (2001) estimate inactivation of VHSV in 15 °C filtered seawater after 60 h at most. Sensitivity of results to changes in the adopted transmissibility parameters is discussed later. We stress that this generalised approach disregards pathogen-specific dilution effects and inactivation rates.

Local and fomite transmission

The final two transmission types are considered to be undirected, and assume an underlying diffusion process, justifying a Gaussian kernel for the decay of risk with distance. They are merely incorporated to add some extra realism. As their effects are deemed to be small, we have chosen parameters that result in low initial likelihoods that, moreover, decrease sharply with distance from the source.

Local transmission involves the movements between sites of staff and other people (e.g. carrying contamination on their clothing, personal items, or private vehicles), as well as local transfer of shared machinery and equipment (nets, containers) (Rodger and Mitchell, 2007; Brennan et al., 2008). The likelihood per day p_{local} is considered to decrease exponentially with radial area around the source site. Given the Euclidean distance D between two sites in meters, average daily transmission rate β and local scalar λ_L, it is defined:

$$p_{local} = \beta \exp\left[-\left(D^2\right)\lambda_L\right].$$

Given the relatively high site density, this type accounts for the large majority of links. However, the transmission likelihood is close to zero for all but the shortest links, and site notification upon detection blocks further spread along this route (Anonymous, 2007). Notification implies a temporary cessation of live fish transports to and from the site, as well as general awareness of an infectious agent on the premises, which should reduce subsequent local spread by increasing general biosecurity measures.

Fomite transmission, the last type of link in our network, represents the uncontrollable part of local transmission, with a daily transmission rate γ and local scalar λ_F, yielding:

$$p_{fomite} = \gamma \exp\left[-\left(D^2\right)\lambda_F\right].$$

Its daily transmission rate is assumed a factor ten less likely than in local transmission due to the haphazard nature of the particle carriers, mainly mammalian predators and scavengers (e.g., otters and foxes) and piscivorous birds (e.g., herons, cormorants, mallards, and sea gulls; McAllister and Owens, 1992; Willumsen, 1989). Another potential threat in this category is posed by eels (*Anguilla anguilla*), which can migrate short distances over land and may carry several fish pathogens, for example VHS and BKD (Chambers et al., 2008; Skall et al., 2005). Fomite transmissions are especially relevant because they cease only when the entire fish stock is culled and the site disinfected. The lower daily likelihood is thus partly offset by a larger window of opportunity, depending on the culling delay.

Model parameterisation

Table 1 lists various properties of the four considered transmission types. To assess the risk of epidemics upon this multi-layered contact structure, our quantified probabilities for each individual connection incorporated empirical contact data and various working assumptions. Both have their limitations. Firstly, regarding empirical data, transports may have been underreported; transmission risk may be underestimated or overlooked (e.g., intra-company transmissions, Sharkey et al., 2008), and circumstances may have changed after the period covered by our data. To maximise the scope of this investigation, we therefore introduced an "outbreak severity" parameter, a global factor with which all transmission probabilities were multiplied (range: 1–10). Increasing this multiplier raises the likelihood of large outbreaks uniformly; it represents increased contact rates, increased infection risks, or a combination of both. For the purposes of risk assessment and the statistical exploration of rare extreme events, pushing the network's epidemic potential by up to an order of magnitude beyond our initial estimates creates a safety margin which we expect the real network never to exceed.

Secondly, regarding working assumptions, daily transmission rates for river, local, and fomite connections are deemed to be small, but their actual values are relatively unknown. In order to ensure reasonable values, we ran a series of tests exploring a range for each parameter, eventually settling on estimates of $\alpha = 0.005$, $\beta = 0.05$, $\gamma = 0.005$, and for the spatial scalars $\lambda_L = 10^{-6}$, and $\lambda_F = 10^{-6}$ (recall that geographical distances are expressed in meters). We subsequently performed extensive sensitivity analyses (see Supplement) by independently varying T, α,β, γ, and the three λ scalars by up to an order of magnitude larger and smaller than their initial estimates. These tests showed that the two undirected transmission types, local and fomite, affected the outbreak size the least, whereas changes in river and especially transport likelihoods had much larger effects. Thus simulation results are most affected by the two probabilities that

Table 1
The four transmission types.

Transmission type	Range	Sources	Receivers	Halted upon	Danger rating
Transport	Unlimited	194	2055	Notification	4
River	Unlimited	596	631	Culling	2
Local	25 km	2089	2089	Notification	1
Fomite	5 km	1577	1577	Culling	1

are empirically best-constrained. In addition, these two types stem from the fewest source sites (see Table 1), suggesting that targeted biosecurity should be highly effective in this network (see Supplement).

Contact structure analysis

The network's contact structure comprises all sites and all potentially infectious links between them. This static structure can be subdivided into clusters of interconnected sites, in which a pathogen introduced at any cluster member can reach any other, either directly or indirectly. Thus a cluster's size imposes an upper bound on the largest outbreak initiated inside it. The more links a network acquires, the higher the likelihood that initially isolated components merge into larger ones. This eventually leads to the formation of the so-called giant component (GC), which incorporates the majority of sites. A GC extended with its sinks (sites that the cluster links into, but not vice versa) is called a giant strongly connected component (GSCC), and constitutes a worst-case scenario of epidemic size for a single infected premises in the absence of control measures (Kao et al., 2006; Dent et al., 2008).

One way to test the robustness of the GSCC is by cumulative removal of links from the contact structure, leading at some point to a fragmentation of the GSCC into smaller clusters that themselves fragment further into isolated sites when even more connections are removed. This procedure not only provides insight into the likelihood of large outbreaks; it may also identify the most dangerous sites from which a pathogen would be able to reach a large part of the network, while most other starting points would leave it trapped in a small subpart of the system. Given the quantified likelihood estimates for transmission contacts on the studied network, we initially chose to explore GSCC fragmentation by systematically removing those links with the lowest transmission rate. Thus we gradually stripped the contact structure of its less likely transmissions, until only the highest-probability contacts remained.

Fig. 4 shows how fragmentation of the network proceeds. At first, almost the entire contact structure is part of the GSCC (red solid line), even when up to half of all connections are severed. At about 60% of structure removed, small clusters start to form, each comprising less than 10% of the network in size (orange dashed line). At over 80% of structure removed, a significant proportion of sites is becoming completely isolated (green dotted line). Above 90% fragmentation the GSCC eventually vanishes, causing a brief spike in small clusters before they themselves also disappear in favour of isolated sites. We repeated this test with randomly selected link removal, yielding the same profile but shifted about 20% rightward, as more of the dense fabric of (low-likelihood) local connections remained active for longer (see Supplement for degree distribution histograms).

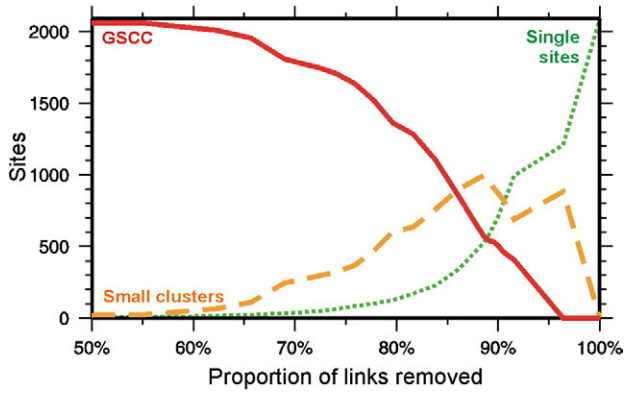

Fig. 4. Fragmentation of the network from a giant, strongly connected component (GSCC, giant component plus sink sites), through an intermediate stage of small clusters, down to single sites, as a lower bound on transmission likelihoods is gradually raised. Lines denote the number of sites that have access to over 90% of the network (red, solid), to less than 10% of it (orange, dashed), or that remain completely isolated (green, dotted).

These progressions show the extreme robustness of the GSCC, highlighting this network's potential to generate large outbreaks. Of particular interest in the first test (removing the lowest likelihoods first) are the 409 sites (including 157 of the 235 fish farms) that maintain access to the GSCC up to the point where the latter collapses. With the large majority of these being situated in dense coastal areas, they tend to have exceptionally many links, including (relatively high-likelihood) transport and river connections, which likely explains their improved access to the GSCC. Increased biosecurity on the outward connections of these highly dangerous spreading sites may be able to prevent a network-wide epidemic from these sources. However, the studied contact structure remains a single, static connectivity snapshot. In order to fully explore the outbreak potential of this network, as well as the efficacy of various control policies, we studied spreading dynamics in large-scale, stochastic, time-dependent epidemiological simulations.

Simulation properties

Delay parameters

The simulator is an automatic event timeline editor driven by stochastics and pre-specified parameters. The timeline functions both as a record of past events, instruction queue for current events, and storage of future events that *may* occur unless control measures cause their removal prior to execution. The sequence of a site's possible states is: *susceptible–infected–infectious–detected (notified)–culled–restocked (=susceptible again)*. A site cannot be re-infected between the stages of *infected* to *restocked*. However, in the course of a single outbreak, a site may become re-infected after becoming susceptible again upon restocking; it may thus partake in spreading dynamics more than once. Furthermore, a site infected with any of the aforementioned notifiable fish diseases is unable to recover naturally without intervention, both in reality and in our simulations.

After the initial infection, inbuilt delays expressed in days (Fig. 5) separate each next step in the sequence. Latency is the duration between becoming infected and becoming infectious to others. The subsequent detection delay ends when authorities are notified that a site is infected and some control measures are implemented. The culling delay is the subsequent period until extermination and removal of hosts, and site disinfection has been carried out, whereas the restocking delay is the imposed ban (fallowing period) before new susceptibles are re-introduced on site. We note that this sequence of states is more detailed than in traditional SEIR models (*susceptible–latent/exposed–infectious–removed/recovered*) where detection induces instantaneous countermeasures.

Together, all possible combinations of the four delay parameters yield one *set* of 2304 separate cases. At runtime, the simulator generates true delays by treating the tabulated values as means to which a truncated Gaussian deviate of ± 2 standard deviations is added to mimic natural variability (Ogut and Bishop, 2007), with one standard deviation equal to 10% of the total value. For example, if the culling delay is 10 days, actual simulated durations between notification and disinfection will be normally distributed between 8 and 12 days (with a mean of 10 days); for the maximum culling delay of 50 days, actual simulated durations would vary from 40 to 60 days.

Timeouts were imposed to limit computational resources spent on essentially endemic outbreaks: the simulated duration was thereto capped at thirty years. Thus any outbreak stopped by timeout was classified as an endemic outbreak, regardless of its size. Existing literature on outbreak duration tends to focus on individual sites, with some estimates ranging from 70 to 141 days on average, and maxima from 168 to 288 days (McLoughlin and Graham, 2007; Rodger and Mitchell, 2007). In combination with the three other delay parameters

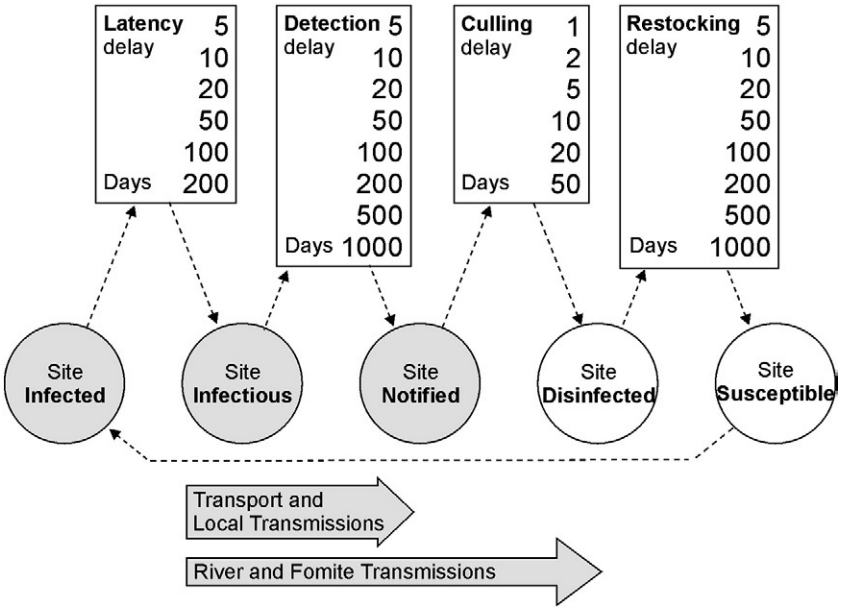

Fig. 5. The modelled sequence of five site states (circles) is interspersed with four delay parameters (rectangles), each one of which can adopt a specific range of values. The variable period between susceptible and infected state (leftward arrow) depends on stochastics and spreading dynamics. Transport and local transmissions from the source site are halted upon detection and notification (fat arrow), but river and fomite transmission continue until the stock has been culled and the site is disinfected (bottom arrow). Shading indicates pathogen presence.

(two of which being of similar magnitude), large simulated outbreaks may easily last more than a decade, prompting consideration of a sufficiently large window of opportunity.

Basic operation

The simulator required a spatial description of sites and a list of all unidirectional links between source-destination pairs, together with the associated type of transmission. For local and fomite links, the Euclidean distance was stored; for river contacts, the distance along the river, and for live fish movements the number of transport contacts per year. At startup, these data were converted into transmission likelihoods for each connection. Simulation then commenced and desired statistics were stored per outbreak and per site. One standard *run* consisted of 10,000 seedings (not all of which necessarily led to larger outbreaks); one standard *set* of all 2304 delay parameter combinations thus totals 23 million seedings.

The simulator initiated each outbreak by infecting a randomly selected site in the otherwise pathogen-free network. The epidemic then progressed as a sequence of chronological events recording time, type of event, and site(s) involved. Event types include infection by any of the four transmission mechanisms (determined randomly according to their respective likelihood), movement from a latent state to an infectious state, notification, culling, and restocking. Additional response events could for example include the imposition or lifting of a national transport ban. Subsequent events were processed until the epidemic had run its course (no more infections or outstanding cullings) or until timeout (set at thirty years). Larger delay parameters may extend an outbreak's duration, but the effect on its size is mixed; longer detection and culling delays extend the window of spreading opportunity, but longer latency may give biosecurity measures more scope, whereas longer restocking delays will limit available susceptible sites within the outbreak's ambit.

Baseline parameters

In order to assess the relative improvement due to various contingency measures, a baseline reference was required. A series of simulations was thereto run of 100,000 seedings each without any control measure in place, and with each outbreak allowed to continue for the maximum duration of thirty years. In the absence of interventions (see Reactive and proactive control strategies), only two parameters remain that affect the results: outbreak severity and latency delay.

Outbreak severity affects the likelihood of hosts becoming infected, the severity of clinical expression, increased transports and other contacts, and less conscientious human behaviour. Here it is incorporated as a global transmission likelihood postfactor (range: 1–10). Initial tests mostly displayed limited outbreaks, so the severity parameter was introduced to push network dynamics gradually towards worse-case scenarios, allowing the performance of specific control measures to be assessed within a range of conditions from innocuous to severe (computational resources permitting). However, we are well aware that reducing such a gamut of aspects to a single multiplier is a simplification (see Discussion).

Estimates of latency delay, the asymptomatic or carrier stage, are documented for a range of fish pathogens. In some species a disease may not express at all (e.g., VHSV in herring, *Clupea harengus*, and sprat, *Sprattus sprattus*) or only at a low, chronic level (Skall et al., 2005; Taylor et al., 2010). In other cases, the latent stage creates an effective reservoir of future problems, resulting in delayed expression or dormancy (Algöet et al., 2009; Smail, 1999). In addition, persistent carrier status may be conferred upon hosts that develop immunity after challenge (Munro et al., 2010); animals will then continue to shed pathogen into their environment while remaining outwardly healthy. In other examples, McLoughlin and Graham (2007) reported subclinical SAV in marine-reared Atlantic salmon, while Tobback et al. (2007) estimated that 25% of asymptomatic trout infected with ERM by immersion actually carried the pathogen in various organs.

Other workers have explored latency at the level of individual hosts (e.g., Ogut and Bishop 2007 for Chinook salmon (*Oncorhynchus tshawytscha*)); however, this study interprets latency at the site population level. In the simulations, a latency delay range was explored from five to two hundred days (Fig. 5). As in the case of the severity postfactor, the aim was not to mimic any particular pathogen, but to explore the epidemiological properties of the English and Welsh network given a range of delay conditions and the type of control measures implemented.

Reactive and proactive control strategies

Three control policies were tested for a variety of relevant parameter settings, namely reactive, proactive, and hybrid controls. Reactive controls assumed that the pathogen clearly and reliably expresses in the hosts after latency, and following some additional delay these clinical signs will be observed, after which further measures are taken. Due to the large timescales of the various delays, the available laboratory processing capacity of detections was deemed inherently capable of keeping up with the number of sites where the pathogen expresses. Thus disease expression drives the response, and the time to detection is directly related to the time of infection.

Contrastingly, proactive controls assumed that the pathogen mostly spreads silently, requiring a programme of dangerous contact tracing after the first detection (the only infection that is detected reactively). In this case, a list was drawn up of all sites directly connected to the infected site, and each was assigned a score based on the danger rating of that connection's transmission type (last column in Table 1; this constitutes a simplification in that individual transmission likelihoods are not accounted for). A large number of regularly-spaced detection slots were then added to the events timeline, based on a new control parameter that defined the number of slots per year (reflecting limited laboratory processing capacity). Only when the simulator encountered the next such slot in the timeline was a particular site selected for analysis, based on the highest danger score in the queue at that time. If this site was also infected, then all its destination sites were added to the queue, with those already present having their cumulative score incremented with the appropriate danger rating. Thus the queuing order could change with each newly detected infection. After a site was processed, it was removed from the queue regardless of the outcome, but it could rejoin it again if one of its connected neighbours was later discovered to be infected.

Given a proactive detection approach, the original detection delay of the first-identified infected site determined the amount of head start the pathogen obtained prior to the engagement of the proactive campaign. In addition, the danger ratings per transmission type of the evaluated connections could affect the outcome, as did the laboratory processing capacity, here defined as the number of reliable assessments of site infection status that can be made within one year.

Aside from field observations of gross pathology, most analyses have to be performed by specialists under controlled conditions in a dedicated facility. Traditional reliable detection involves culturing the suspected pathogen on a suitable medium or cell line, which may take weeks to months (e.g., 1–3 weeks for IPNV, up to 10 weeks for BKD; Chambers et al., 2008; Munro et al., 2010). For other pathogens (e.g. GS), identification is based on examination of morphological features. Histopathology may also provide a provisional diagnosis and can be relatively rapid (less than 48 h) but is dependent on the skill of the pathologist. More recent swift methods include immunodiagnostics (serological tests for antigens in a host) and molecular genetics (notably polymerase chain reaction) to detect and identify part of a pathogen's nucleic acid sequence.

Laboratory capacity in the simulations ranged from ten to five hundred conclusive site tests per year (likely shared among multiple facilities, although no formal agreements to that effect are currently in place). The purpose was not to match current processing capacity within England and Wales, but to explore the response of the entire system when this parameter is varied by over an order of magnitude. We note that the related constraints of limited field staff and pathogen-specific resource requirements were not taken into account.

Hybrid control strategy

The third, hybrid strategy combines reactive and proactive controls. It can represent either of two disease scenarios: an intermediate type of pathogen that expresses clinical symptoms sometimes, but too infrequently to enable complete reliance on a reactive control policy, or alternatively, a pathogen that does express reliably in hosts (like in the reactive case), with contact tracing providing an additional mitigation effort. Since this strategy is labour-intensive and imposes large demands on laboratory capacity, yet may produce a significant number of negative test results for uninfected sites, its efficacy in these situations was considered of interest for policy makers deciding on the type of resources to allocate.

Unlike the proactive case, where contact tracing is the only way to track a silently spreading pathogen, the hybrid strategy represents a choice of different emphases, on either the reactive or the proactive part of the strategy. The detection queue was thereto filled on the basis of both the (reactive) detection delay *and* (proactive) dangerous contact tracing. We explored different ratios between reactive and proactive detection analyses, in particular to determine to what extent additional dangerous contact tracing could prevent an outbreak from escaping the initial seeding area. This differs from the more realistic strategy that would always process all reactive detections preferentially. Tested ratios are: [1/1], [2/1], [5/2], [5/1], [10/1], and their inverse, yielding nine cases.

Detection slots were regularly distributed along the timeline as in the proactive case, but whenever the simulator processed such a slot, it first incremented a step counter in a cyclical array that determined whether to order the queue chronologically (providing the time of pathogen expression had already been reached for the top site; if not, a proactive detection was performed), or ranked by cumulative danger rating, as in the purely proactive case. Given a specified number of reactive and proactive detections per cycle, their slots were distributed as evenly as possible. If a site first entered the queue as a destination of a reactively detected source, it received an initial danger rating of unity (lowest on the scale); its rating could subsequently increase due to the proactive policy. Thus both accumulated danger ranking and detected clinical expression could determine the time of laboratory processing.

Additional control measures

The effects of two special control measures were explored. The simplest of these is the national transport ban (e.g., the Scottish contingency plan for GS includes scope for such a measure). The day after a pathogen is detected at the first site, all transports are disabled on the entire network for thirty days. Moreover, whenever a new site is found to be infected while this prohibition is in force, the ban expiry clock is reset to zero. Only when the ban duration is completed without any new detections of infected sites are transports allowed again, until the next detected infection imposes a new national ban. This measure was tested on proactive and reactive control policies. Less drastic interventions (e.g., transport restrictions at the catchment level, or within some given radius around a notified site) we leave for future work; here the aim was to provide an indication of maximum achievable benefit.

The second additional strategy is a public campaign by authorities to warn site owners of a new outbreak (McLaws et al., 2007). Such increased awareness of a particular pathogen's presence in the community was deemed to reduce all subsequent detection delays by half, relative to the initial one. The awareness campaign was tested on the reactive policy only, as silently spreading pathogens render increased vigilance useless. This policy differs from the spreading awareness of human disease as explored by Funk et al. (2009), who reduced susceptibility of infection as a function of available, high-quality information which itself spread through the network. In fish diseases, however, infection susceptibility of the animal hosts was deemed to remain unaffected by the mere awareness among human operators of potential pathogen presence. Instead, the likelihood of earlier detection of advertised clinical signs seemed a more realistic effect to explore in this context.

Table 2
Tested control strategies.

Strategy	Cases	Severity	Lab capacity per year	Other parameters
Reactive	24	1, 2, 3, 4, 5, 10	Unlimited	National Transport Ban Awareness Campaign
Proactive	72	1, 2, 3, 4, 5, 10	10, 20, 50, 100, 200, 500	National Transport Ban
Hybrid	54	5	10, 20, 50, 100, 200, 500	Proactive/reactive ratio

Combining all relevant parameter choices for each control policy and additional measures yielded 150 separate cases (Table 2). Each case was explored with a full set of delay parameters, requiring about 3.5 billion seedings in total. Within each policy, the experimental design is fully balanced. However, computational limitations forced some differences in the parameters explored between the three main strategies. For example, in the hybrid policy, six choices of laboratory capacity and nine possible combinations of proactively and reactively selected sites to analyse yielded 54 permutations, which would increase six-fold if the full spectrum of severity had been considered; instead we chose a fixed factor of 5 here.

Results

Outbreak size under different control policies

The baseline cases (exploring severity and latency delay only) represent a benchmark of worst-case scenarios. All outbreaks were unrealistically allowed to continue for the maximum duration of thirty years without any intervention. Thus once infected, a site remained so until timeout. Given medium-high severity (factor 5) and averaged over all six latencies, the average outbreak size is 132.6 sites, whereas the maximum exceeds three quarters of the network infected. However, one could argue more optimistically that given lowest severity, up to three quarters of the network is still pathogen-free after thirty years. Severity is by far the most important parameter here; only the largest latency delays have some effect in reducing outbreak sizes by slowing down spreading (Fig. 6).

By contrast, all control policies produce much smaller outbreaks. Comparing average outbreak sizes under the same medium-high severity condition as before and averaged over all delay parameter permutations and lab capacities, the reactive strategy yields 5.9 sites, and the proactive 10.9, whereas the hybrid (with equal division of reactive and proactive detections) performs best with 4.9 sites. The hybrid policy also limits the average duration of outbreaks (508 days, against 732 and 860 for reactive and proactive controls respectively) and the average number of endemic outbreaks (42.7 per 10,000, against 131.4 for the reactive and 146.1 for the proactive strategy). However, limited laboratory capacity causes proactive and hybrid controls to perform substantially worse in the case of the largest outbreaks, with maximum outbreak sizes of 1114 and 739 respectively (when averaged over all six tested laboratory capacity settings), against a mere 195 for the reactive policy.

The reactive policy allowed two additional control methods to be evaluated: a national Transport Ban (TB, 30 days plus extensions), and a public awareness campaign (AC, reducing detection delays after the first case by half). Averaging response variables over one entire set (2304 times 10,000 seedings, severity factor 5), AC and TB are similarly effective in reducing average outbreak size from 5.9 to 2.6 and 2.7 sites respectively. The maximum outbreak size is reduced from 195 sites to 85 (AC) and 74 (TB), and the number of endemic outbreaks from 131 sites to 54 (AC) and 100 (TB). The outbreak duration is unchanged by the TB (736 days against 732 originally), but reduced by the AC (645). Thus the TB performs best at the high end of the outbreak spectrum, whereas the AC does better overall.

These two measures can also be applied together, yielding outbreak sizes of 1.9 (average) and 46 (max.), while the number of endemic outbreaks drops to 41; outbreak duration remains as for AC alone (634 days). Given a proactive strategy (all six laboratory capacity choices combined; sample size: 6 times 2304 times 10,000 seedings), the TB again reduces outbreak size by more than half, the average from 10.9 to 4.6 sites, the maximum from 1114 to 468. Lastly, the average number of endemic outbreaks shrinks from 146 to 118 while the

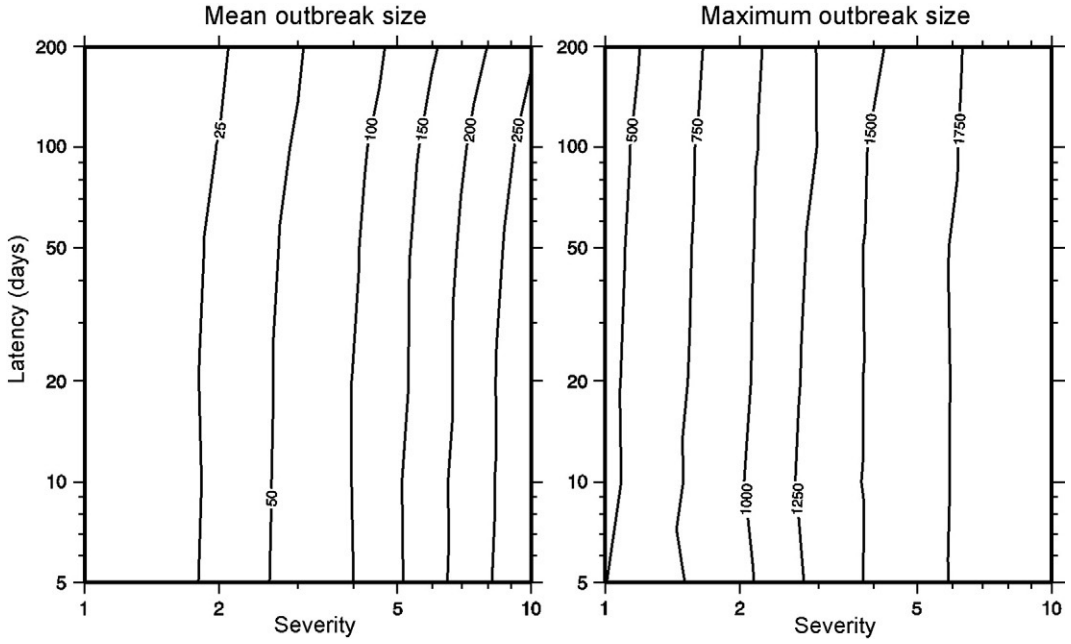

Fig. 6. Baseline results (average outbreak size on left, maximum outbreak size on right, and log–log scale) for different choices of latency delay and outbreak severity are mainly affected by the latter (36 permutations per plot; 100,000 seedings per run, each allowed to spread for 30 years without intervention).

average outbreak duration remains unchanged. We stress that these values should be interpreted merely as relative measures of system response, not as absolute predictions of real outbreaks.

Transmission types, site types, and geographic risk

Concerning transmission paths, the proportional representation of the four types is highly uneven (see Supplement). Assessing all severity cases together, between 50 and 60% of transmissions in the reactive case were local, with fomites accounting for another 10%, and river and transport being responsible for 10–20% and 20% respectively. These percentages are sharp peaks in unimodal distributions with thin tails. In the proactive case, the peaks for fomite and river transmissions are somewhat broader, but local and transport were bimodal with peaks at 20 and 50%. Separate unimodal distributions are recovered when results are split by severity, which shows that for maximum severity the proportion of transport transmissions rises dramatically (to ca. 65% of the total), mostly at the cost of local transmission. This transition is possibly due to the much larger typical outbreak sizes for higher severities, which allow more of the few, dispersed transport source sites (fish farms) to come into play. A temporal explanation (longer-lasting outbreaks allowing more transports to accumulate over time) is less likely, as severity was found to have little effect on outbreak duration.

In terms of site types, the 235 fish farms and 1855 fisheries should be considered as two different entities, both in network architecture and recorded transmissions. All transport connections originated at fish farms, and these sites also tend to reside in areas with a higher site density, increasing their local and fomite infection routes. Moreover, nonparametric Kruskal–Wallis tests showed that outward transport and inward transport and river transmissions represent most of the significant differences between the two site types. From a biosecurity perspective, fish farms can thus be seen as high-risk sources, both to other fish farms (via transport and river contacts) and to fisheries (via transport), whereas fishery sites are primarily at risk as receivers of pathogens.

For specific parameter choices, stored transmission totals per site yielded geographic risk maps per catchment (see Supplement). Fig. 7 shows an example for the proactive policy with medium-high severity (factor 5) and medium delays. Most notable is the clear distinction between the map of sources (left panel, more concentrated) and that of receivers (right panel). Furthermore, although absolute transmissions are lower in the other two policies, the same highest-risk catchments are identifiable in all, which do not necessarily coincide with high site density (Fig. 1).

Significance of specific parameters

We investigated which parameters affect which response variables most, and at which level, using statistical ANalysis Of VAriance (ANOVA). To exploit its full potential, we adopted a balanced design, i.e., within each control policy the number of simulations was equal for each combination of parameter levels (full results in Supplement). We then divided seven response variables into two "meta-response" groups, and ranked ANOVA-derived parameter contributions to a response by size. The first such group expresses the severity of outbreaks; it contains average and maximum outbreak size and the number of endemic outbreaks. Given reactive controls, this meta-response is most affected by the detection delay, followed by severity and (at distance) the AC; remaining parameters had little effect. In the proactive case, detection and severity share top ranking, followed by the laboratory capacity, culling delay, and TB; restocking and latency delay close the ranks. If applying a hybrid policy, laboratory capacity is the most important parameter, followed by the detection delay. Culling and latency then provide modest, roughly equal contributions, and the applied reactive/proactive ratio is last. The restocking delay again appears to have little effect.

The second meta-response contains the average outbreak duration, the length of the processing queue, and the number of negative test results. The reactive policy yields the simplest profile: detection delay is most important, now followed by latency; all other parameters have little effect. The proactive strategy ranks laboratory capacity first, followed by culling, detection, and severity; remaining parameters contribute little. Lastly, in the hybrid case, the culling delay rates highest, followed by equal contributions from detection and laboratory capacity. The rota ratio and latency close the ranks.

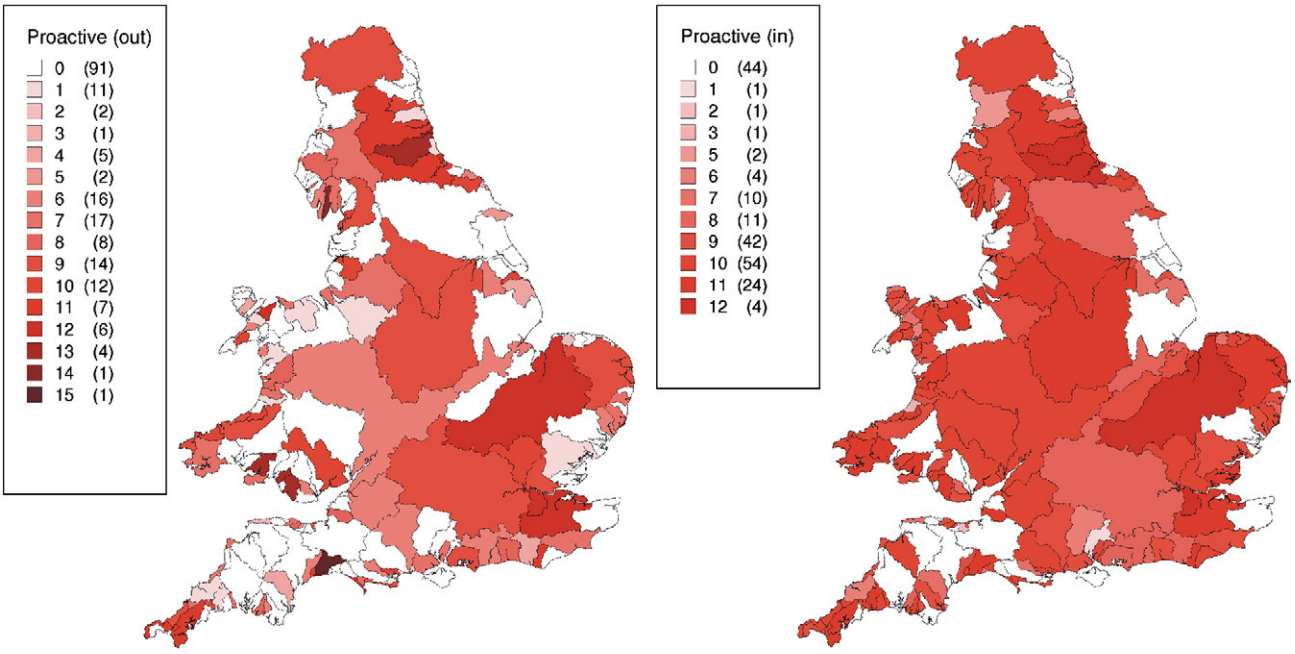

Fig. 7. Geographic risk distribution per catchment, for the proactive policy. *Left*: outward transmissions. *Right*: inward transmissions. Colour scale: site transmission totals, averaged per catchment, log-transformed, in equal-width bins (number of catchments in brackets).

The importance of rapid response in terms of brief detection and culling delays that is apparent from these results is itself unsurprising and in agreement with earlier studies (e.g., Haydon et al., 1997; Fraser et al., 2004), but also differs from these in several respects. Firstly, information is gained when these two delays are distinguished from one another, rather than taken together in a single "infectious" state, as in SIR and SEIR models. This is underlined by the culling delay being more important (Howard and Donnelly, 2000) than detection delay in the hybrid policy, but relatively unimportant in the reactive policy. Secondly, neither delay is necessarily *always* the most important factor; in specific circumstances, laboratory capacity can be more decisive. Thirdly, balanced ANOVA yields the statistically significant estimates of importance of each considered parameter in each studied scenario (see Supplement), quantifying their contribution to a number of response variables with respect to all others considered, yielding more solid grounds for their assessment.

Finally, the largest outbreaks appear to occur mostly due to the interplay of several factors and circumstances. In terms of contact structure, a crucial difference with many other epidemiological networks and models is the absence of a large majority of sites with few connections. In the most serious outbreaks, the observed dense mesh of links (especially in coastal regions) causes contact tracing to be simply overwhelmed with too many potentially threatened sites that turn out to test negative, wasting the large majority of laboratory capacity. This also implies that some infected sites are processed too late (after having already transmitted the pathogen to many neighbours near and far) or are missed entirely when the most active infection front temporarily moves elsewhere (causing a shift in queuing priorities). The latter situation enabled repeated "flare-ups" of new infection pressure from seeding areas that otherwise displayed prolonged reduced transmission activity.

A second set of factors concerns transport and river connections, which are directed, frequently long-distance (creating the small-world effect), and have a relatively high transmission likelihood. Transport sources (fish farms) in particular are few, but reside in the densest areas and service virtually the entire network. In combination with the more clustered river links, the fish farms appear to function as a spreading amplification system. They provide not just quick access to distant parts of the network, but their dense interlinking provides numerous opportunities for feedback, that is, once a pathogen infects a fish farm, chances rise markedly that multiple connected fish farms will reinforce its spreading by repeated mutual infection within their sub-network, as well as ensuring distribution among each one's community of dependent fishery sites, which may in turn act as long-term background reservoir. Together, these factors conspire to pose enduring challenges for effective control in these worst-case scenarios.

Discussion

The main purpose of this effort was to explore epidemiological network responses in multi-dimensional parameter space, to identify the most influential factors and countermeasures to reduce the severity of disease outbreaks. In this context, an important feature of the studied network is the directed nature of river and transport connections, which has clear implications for targeted biosecurity measures. In addition, the highly skewed ratio of transport sources versus receivers (Table 1) implies that the former may be targeted more economically than the latter.

The balanced design of the simulation experiment ensured the internal consistency of results within each of the three main control policies tested. However, the previous section should not be interpreted as a scoreboard of competing strategies, since each represents a specific situation. The reactive policy applies to pathogens that clinically express themselves quickly and reliably, and also assumes that surveillance is adequate and laboratory capacity is ample; the proactive policy instead presupposes silent spreading with limited testing resources; the hybrid policy resides somewhere in between. None is *a priori* best.

Likewise, the two additional measures operate along different lines. The public awareness campaign (AC) targets the entire network; the associated efficacy assumption of subsequent reduction of all detection delays by half is probably too optimistic, and certainly a simplification (McLaws et al., 2007; Funk et al., 2009; Fraser et al., 2004). The national transport ban (TB) affects almost the entire network in terms of receivers, but targets only a small fraction of sources. However, prolonged movement controls would be extremely damaging to the industry. Furthermore, ANOVA has shown AC to be a more influential instrument than TB when the entire spectrum of outbreak sizes is considered, whereas TB appears most effective in reducing the largest outbreaks. Given that the latter are rare, a public awareness campaign may therefore be a more acceptable alternative.

Caveats

In assessing the ANOVA results, it is important to distinguish those factors that can be controlled, those that cannot, and those that are principally unknown. Outbreak severity largely escapes human control (aside from aiming to reduce stress levels in fish populations) and can be assayed only retrospectively, or *in vitro* per species, which lacks some relevant *in vivo* conditions. Numerous real factors may be involved, such as different strains of the pathogen, environmental conditions (e.g., water temperature, pH, salinity, and pollutants), variable susceptibility of different fish species, and the genetic, immune, and physiological condition of individual hosts (Feist et al., 2002; McLoughlin and Graham, 2007; Tobback et al., 2007; Chambers et al., 2008; Peeler et al., 2008; Algöet et al., 2009). Their effects and interactions are only partially understood and poorly quantified.

Latency delay is likewise beyond control and poorly understood, but unlike severity, its effects appear limited in our simulations, possibly even beneficial from a control standpoint in acting as an extra delay on the spreading dynamics, allowing more time for biosecurity measures such as contact tracing (Kiss et al., 2005, 2006a).

Another area of concern involves the various interactions between wild and cultured fish. Introducing wild fish as potential carriers adds several complications: they may become infected through direct exposure to pathogens released by farmed populations or through predation on infected stocked or escaped fish. For example, wild species in the vicinity of infected sites can show up to an order of magnitude higher prevalence of that infection than elsewhere (e.g. IPNV, Wallace et al., 2008; sea lice, Krkošek et al., 2007). Wild fish can also move independently in search of food, mates, and shelter, increasing the risk of exposure and subsequent spread of disease. Furthermore, diadromous fish periodically migrate upstream and have the potential to introduce infections from the marine environment to freshwater populations (Skall et al., 2005; Stone et al., 2008). Wild freshwater species may also act as a permanent reservoir of disease, maintained partly through vertical transmission (parent to offspring). For example, grayling (*Thymallus thymallus*) is highly susceptible to LG and BKD infections, and the latter was found to be associated with BKD-infected rainbow trout farms within the same river catchment (Chambers et al., 2008; Algöet et al., 2009).

Cultured populations may themselves also act as pathogen reservoirs. For example, the prevalence of BKD is generally higher in cultured fish than in the wild (Nowak and LaPatra, 2006; Chambers et al., 2008); Gregory et al., 2007 reported IPNV having been isolated from a variety of European marine reservoirs (wild fish, mussels, prawns, crabs, and sediments) in the vicinity of fish farms; Krkošek et al. (2007, 2009) identified prolonged exposure of juvenile wild salmon to sea lice as associated with nearby commercial salmon farms; and McLoughlin and Graham (2007) considered pancreas disease (SAV) to be endemic in most salmon marine sites in Ireland, and in other countries on sites with a history of infection. In addition,

transmission mechanisms here include direct contact through freshwater cages and fish escaping due to a failure in containment (e.g., during a flood). We leave these various issues for future work.

Concluding remarks and guidelines

Despite the listed caveats, our generalised, simplified simulations did yield some robust conclusions. Regardless of which policy is pursued, the analyses demonstrated that detection delay is the most influential control parameter overall for the studied outbreak dynamics. This importance likely also feeds into the success of the public awareness campaign (which expedites detection). Clearly, government agencies and the industry alike have valuable roles to play here, in constant surveillance, sampling programmes, record keeping, and collaboration. The main problem is that the duration in question is difficult to quantify in the absence of observed timing of the initial introduction of the pathogen on site. Only in the case of live fish transports, and possibly local spread, may a direct causal connection be established in hindsight; the other two transmission types involve numerous factors too ephemeral to detect, let alone quantify. What we can do, however, is to approach them statistically. The river flow stream analysis is a case in point, revealing rapid transits.

Of the remaining delay parameters, the restocking delay appears to be least important. The culling delay, by contrast, is an influential control, as is the available laboratory capacity, which becomes increasingly significant in larger and longer-lasting epidemics. Finally, if pursuing a hybrid strategy, each reactive detection should be processed as soon as possible; only spare laboratory capacity should be spent on dangerous contact tracing.

We close this discussion with a few quantitative guidelines derived from the simulations. We stress that these conclusions are based upon our synthetic, simplified representations of reality that incorporate numerous assumptions that may not fully match the actual, ever-changing situation. Moreover, these models do not aim to mimic a specific pathogen with particular infection characteristics; pathogen-specific simulations, in combination with information from other sources, would be required to produce disease-specific recommendations. However, by exploring parameter space in many orthogonal directions, using the most recent available empirical description of the real network, obtaining large samples, and tuning multiple scenarios to achieve the entire gamut from harmless to devastating outbreaks, we hope that we have captured the essence of this network that transcends studies of individual cases and pathogens.

The presented guidelines are derived from so-called main effects plots. A main effect occurs when a response variable's mean changes significantly across the levels of a considered parameter (see Supplement). Within a progression of discrete parameter levels, one can thereby identify the bound beyond which the response would on average exceed its overall mean. Thus the criterion in all cases is to restrict responses to better-than-average as computed over all observations. Whether these limits are practically acceptable is debatable; we also note that actual individual epidemics may still exceed them. The various estimates can be distilled into the following general guidelines:

- keep the detection delay below 200 days (below 100 days in the proactive case, where it refers to detection of the first case only);
- keep laboratory capacity above 100 conclusive site tests per year;
- keep the culling delay below 20 days (below 10 days in the hybrid case);
- keep the restocking delay above 200 days.

Lastly, we reiterate some of the findings stated elsewhere in the text:

- the detection delay is the most important parameter within human control, followed by laboratory capacity and culling delay;
- no English or Welsh river transit time or associated river distance between two sites is beyond a fish pathogen's potential survival range;
- fish farms and fisheries are different entities, requiring distinct biosecurity measures;
- outward and inward transmission risk should be assessed separately.

Supplementary data to this article can be found online at doi: 10.1016/j.epidem.2010.08.001.

Acknowledgments

We gratefully acknowledge the support of: the Department for Environment, Food, and Rural Affairs (Defra) who funded this work; the Centre for Ecology and Hydrology (CEH) for assistance with generation of inter-node distances between farms and fisheries for the river contact network; the United States Geological Survey (USGS) for providing a large sample of river stream flow speed measurements in their public water resources database at http://waterdata.usgs.gov/usa/nwis; I.C. Smith at the University of Liverpool, United Kingdom, for assistance with high-throughput computing (Condor); and two anonymous referees, who suggested numerous improvements.

References

Algöet, M., Bayley, A.E., Roberts, E.G., Feist, S.W., Wheeler, R.W., Verner-Jeffreys, D.W., 2009. Susceptibility of selected freshwater fish species to a UK *Lactococcus garvieae* isolate. J. Fish Dis. 32, 825–834. doi:10.1111/j.1365-2761.2009.01058.x.

Anonymous, 1975. Salmon and Freshwater Fisheries Act 1975. Stationery Office, London.

Anonymous, 2007. Bacterial kidney disease: detection and control in Great Britain. CEFAS Finfish News 4, 5–11.

Barja, J.L., Toranzo, A.E., Lemos, M.L., Hetrick, F.M., 1983. Influence of water temperature and salinity on the survival of IPN and IHN viruses. Bull. Europ. Assoc. Fish Pathol. 3 (4), 47–50.

Bigras-Poulin, M., Barfod, K., Mortensen, S., Greiner, M., 2007. Relationship of trade patterns of the Danish swine industry animal movements network to potential disease spread. Prev. Vet. Med. 80, 143–165.

Brennan, M.L., Kemp, R., Christley, R.M., 2008. Direct and indirect contacts between cattle farms in north-west England. Prev. Vet. Med. 84, 242–260.

Chambers, E., Gardiner, R., Peeler, E.J., 2008. An investigation into the prevalence of *Renibacterium salmoninarum* in farmed rainbow trout, *Oncorhynchus mykiss* (Walbaum), and wild fish populations in selected river catchments in England and Wales between 1998 and 2000. J. Fish Dis. 31, 89–96.

Christley, R.M., Robinson, S.E., Lysons, R., French, N.P., 2005. Network analysis of cattle movement in Great Britain. In: Mellor, D.J., Russell, A.M., Wood, J.L.N. (Eds.), Proc. Soc. Vet. Epidem. Prev. Med. Nairn, Scotland, pp. 234–244.

Damsgård, B., Mortensen, A., Sommer, A.-I., 1998. Effects of infectious pancreatic necrosis virus (IPNV) on appetite and growth in Atlantic salmon, *Salmo salar* L. Aquaculture 163, 185–193.

Dent, J.E., Kao, R.R., Kiss, I.Z., Hyder, K., Arnold, M., 2008. Contact structures in the poultry industry in Great Britain: Exploring transmission routes for a potential avian influenza virus epidemic. BMC Vet. Res. 4 (27): 1-14.

Feist, S.W., Peeler, E.J., Gardiner, R., Smith, E., Longshaw, M., 2002. Proliferative kidney disease and renal myxosporidiosis in juvenile salmonids from rivers in England and Wales. J. Fish Dis. 25, 451–458.

Food and Agriculture Organisation of the United Nations, 2004. The State of World Fisheries and Aquaculture (SOFIA), p. 153.

Food And Agriculture Organisation of the United Nations, Network of Aquaculture Centres in Asia, 2001. Manual of the procedures for the implementation of the Asia Regional Technical Guidelines on Health Management for the Responsible Movement of Live Aquatic Animals. FAO Fisheries Technical Paper 402/1.

Fraser, C., Riley, S., Anderson, R.M., Ferguson, N.M., 2004. Factors that make an infectious disease outbreak controllable. Proc. Nat. Acad. Sci. 101 (16), 6146–6151.

Funk, S., Gilad, E., Watkins, C., Jansen, V.A.A., 2009. The spread of awareness and its impact on epidemic outbreaks. Proc. Nat. Acad. Sci. 106 (16), 6872–6877.

Giorgetti, G., 1998. The cost of disease. FAO EastFish Mag. 1, 40–41.

Green, D.M., Gregory, A., Munro, L.A., 2009. Small- and large-scale network structure of live fish movements in Scotland. Prev. Vet. Med. 91 (2–4), 261–269. doi:10.1016/j.prevetmed.2009.05.031.

Gregory, A., Munro, L.A., Wallace, I.S., Bain, N., Raynard, R.S., 2007. Detection of infectious pancreatic necrosis virus (IPNV) from the environment in the vicinity of IPNV-infected Atlantic salmon farms in Scotland. J. Fish Dis. 30, 621–630.

Gustafson, L.L., Ellis, S.K., Beattie, M.J., Chang, B.D., Dickey, D.A., Robinson, T.L., Marenghi, F.P., Moffett, P.J., Page, F.H., 2007. Hydrographics and the timing of infectious salmon anemia outbreaks among Atlantic salmon (*Salmo salar* L.) farms in the Quoddy region of Maine, USA and New Brunswick. Canada. Prev. Vet. Med. 78, 35–56.

Hattenberger Baudouy, A.M., Danton, M., Merle, G., de Kinkelin, P., 1995. Epidemiology of Infectious Hematopoietic Necrosis (IHN) of salmonid fish in France: study of the course of natural infection by combined use of viral examination and seroneutralization test and eradication attempts. Vet. Res. 26, 256–275.

Haydon, D.T., Woolhouse, M.E.J., Kitching, R.P., 1997. An analysis of foot-and-mouth-disease epidemics in the U.K. IMA J Math. Appl. Med. Biol. 14, 1–9.

Howard, S.C., Donnelly, C.A., 2000. The importance of immediate destruction in epidemics of foot and mouth disease. Res. Vet. Sci. 69, 189–196. doi:10.1053/rvsc.2000.0415.

Iversen, M., Finstad, B., McKinley, R.S., Eliassen, R.A., Carlsen, K.T., Evjen, T., 2005. Stress responses in Atlantic salmon (*Salmo salar* L.) smolts during commercial well boat transports, and effects on survival after transfer to sea. Aquaculture 243 (1–4), 373–382. doi:10.1016/j.aquaculture.2004.10.019.

Jonkers, A.R.T., Sharkey, K.J., Christley, R.M., 2010. Preventable H5N1 avian influenza epidemics in the British poultry industry network exhibit characteristic scales. J. R. Soc. Interface 7 (45), 695–701. doi:10.1098/rsif.2009.0304.

Kao, R.R., Danon, L., Green, D.M., Kiss, I.Z., 2006. Demographic structure and pathogen dynamics on the network of livestock movements in Great Britain. Proc. R. Soc. B 273, 1999–2007. doi:10.1098/rspb.2006.3505.

Keeling, M.J., 1999. The effects of local spatial structure on epidemiological invasions. Proc. R. Soc. B 266, 859–867. doi:10.1098/rspb.1999.0716.

Kiss, I.Z., Green, D.M., Kao, R.R., 2005. Disease contact tracing in random and clustered networks. Proc. R. Soc. B 272, 1407–1414. doi:10.1098/rspb.2005.3092.

Kiss, I.Z., Green, D.M., Kao, R.R., 2006a. Infectious disease control using contact tracing in random and scale-free networks. J. R. Soc. Interface 3, 55–62. doi:10.1098/rsif.2005.0079.

Kiss, I.Z., Green, D.M., Kao, R.R., 2006b. The effect of contact heterogeneity and multiple routes of transmission on final epidemic size. Math. Biosci. 203, 124–136.

Kocan, R.M., Hershberger, P.K., Elder, N.E., 2001. Survival of the north American strain of viral hemorrhagic septicemia virus (VHSV) in filtered seawater and seawater containing ovarian fluid, crude oil, and serum-enriched culture medium. Dis. Aq. Organ. 44, 75–78.

Krkošek, M., Ford, J.S., Morton, A., Lele, S., Myers, R.A., Lewis, M.A., 2007. Declining wild salmon populations in relation to parasites from farm salmon. Science 318, 1772–1775.

Krkošek, M., Morton, A., Volpe, J.P., Lewis, M.A., 2009. Sea lice and salmon population dynamics: effects of exposure time for migratory fish. Proc. R. Soc. B 276, 2819–2828. doi:10.1098/rspb.2009.0317.

LaPatra, S.E., Batts, W.N., Overturf, K., Jones, G.N., Shewmaker, W.D., Winton, J.R., 2001. Negligible risk associated with the movement of processed rainbow trout, *Oncorhynchus mykiss* (Walbaum), from an infectious haematopoietic necrosis virus (IHNV) endemic area. J. Fish Dis. 24 (7), 399–408. doi:10.1046/j.1365-2761.2001.00316.x.

Lilley, J.H., Roberts, R.J., 1997. Pathogenicity and culture studies comparing the Aphanomyces involved in epizootic ulcerative syndrome (EUS) with other similar fungi. J. Fish Dis. 20, 135–144.

McAllister, P.E., Bebak, J., 1997. Infectious pancreatic necrosis virus in the environment: relationship to effluent from aquaculture facilities. J. Fish Dis. 20, 201–207.

McAllister, P.E., Owens, W.J., 1992. Recovery of infectious pancreatic necrosis virus from the faeces of wild piscivorous birds. Aquaculture 106, 227–232.

McLaws, M., Ribble, C., Stephen, C., McNab, B., Barrios, P.R., 2007. Reporting of suspect cases of foot-and-mouth-disease during the 2001 epidemic in the U.K., and the herd sensitivity and herd specificity of clinical diagnosis. Prev. Vet. Med. 78 (1), 12–23. doi:10.1016/j.prevetmed.2006.09.001.

McLoughlin, M.F., Graham, D.A., 2007. Alphavirus infections in salmonids: a review. J. Fish Dis. 30, 511–531.

Moore, C., Newman, M.E.J., 2000. Epidemics and percolation in small-world networks. Phys. Rev. E 61 (3), 5678–5682.

Munro, L.A., Gregory, A., 2009. Application of network analysis to farmed salmonid movement data from Scotland. J. Fish Dis. 32, 641–644. doi:10.1111/j.1365-2761.2009.01076.x.

Munro, E.S., Millar, C.P., Hastings, T.S., 2010. An analysis of levels of infectious pancreatic necrosis virus in Atlantic salmon, *Salmo salar* L., broodstock in Scotland between 1990–2002. J. Fish Dis. 33, 171–177. doi:10.1111/j.1365-2761.2009.01114.x.

Murray, A.G., 2006. A model of the emergence of infectious pancreatic necrosis virus in Scottish salmon farms, 1996–2003. Ecol. Modell. 199, 64–72.

Murray, A.G., Peeler, E.J., 2005. A framework for understanding the potential for emerging diseases in aquaculture. Prev. Vet. Med. 67, 223–235.

Murray, A.G., Smith, R.J., Stagg, R.M., 2002. Shipping and the spread of infectious salmon anemia in Scottish aquaculture. Emerg. Infect. Dis. 8, 1–5.

Murray, A.G., Amundrud, T.L., Gillibrand, Ph.A., 2005. Models of hydrodynamic pathogen dispersal affecting Scottish salmon production: modelling shows how Scotland eradicated ISA, but not IPN. Bull. Aquacult. Assoc. Can. 105-1, 79–86.

Nowak, B.F., LaPatra, S.E., 2006. Epitheliocystis in fish. J. Fish Dis. 29, 573–588.

Ogut, H., Bishop, S.C., 2007. A stochastic modelling approach to describing the dynamics of an experimental furunculosis epidemic in Chinook salmon, *Oncorhynchus tshawytscha* (Walbaum). J. Fish Dis. 30, 93–100.

Peeler, E.J., Thrush, M.A., 2004. Qualitative analysis of the risk of introducing *Gyrodactylus salaris* into the United Kingdom. Dis. Aquat. Organ. 62, 103–113.

Peeler, E.J., Feist, S.W., Longshaw, M., Thrush, M.A., St-Hilaire, S., 2008. An assessment of the variation in the prevalence of renal myxosporidiosis and hepatitis in wild brown trout, *Salmo trutta* L., within and between rivers in South-West England. J. Fish Dis. 31, 719–728. doi:10.1111/j.1365-2761.2008.00942.x.

Rodger, H., Mitchell, S., 2007. Epidemiological observations of pancreas disease of farmed Atlantic salmon, *Salmo salar* L., in Ireland. J Fish Dis 30, 157–167.

Sharkey, K.J., 2008. Deterministic epidemiological models at the individual level. J. Math. Biol. 57, 311–331. doi:10.1007/s00285-008-0161-7.

Sharkey, K.J., Fernandez, C., Morgan, K.L., Peeler, E.J., Thrush, M.A., Turnbull, J.F., Bowers, R.G., 2006. Pair-level approximations to the spatio-temporal dynamics of epidemics on asymmetric contact networks. J. Math. Biol. 53, 61–85. doi:10.1007/s00285-006-0377-3.

Sharkey, K.J., Bowers, R.G., Morgan, K.L., Robinson, S.E., Christley, R.M., 2008. Epidemiological consequences of an incursion of highly pathogenic H5N1 avian influenza into the British poultry flock. Proc. R. Soc. B 275 (1630), 19–28.

Skall, H.F., Olesen, N.J., Mellergaard, S., 2005. Viral haemorrhagic septicaemia virus in marine fish and its implications for fish farming: a review. J. Fish Dis. 28, 509–529.

Smail, D.A., 1999. Viral haemorrhagic septicaemia. In: Woo, P.T.K., Bruno, D.W. (Eds.), Fish Diseases and Disorders. Vol 3: Viral, Bacterial and Fungal Infections. CABI, Wallingford, pp. 123–147.

Stone, D.M., Ferguson, H.W., Tyson, P.A., Savage, J., Wood, G., Dodge, M.J., Woolford, G., Dixon, P.F., Feist, S.W., Way, K., 2008. The first report of viral haemorrhagic septicaemia in farmed rainbow trout, *Oncorhynchus mykiss* (Walbaum), in the United Kingdom. J. Fish Dis. 31, 775–784. doi:10.1111/j.1365-2761.2008.00951.x.

Taylor, N.G.H., Dixon, P.F., Jeffery, K.R., Peeler, E.J., Denham, K.L., Way, K., 2010. Koi herpesvirus: distribution and prospects for control in England and Wales. J. Fish Dis. 33, 221–230. doi:10.1111/j.1365-2761.2009.01111.x.

Thrush, M., Peeler, E., 2006. Stochastic simulation of live salmonid movement in England and Wales to predict potential spread of exotic pathogens. Dis. Aquat. Organ. 72, 115–123.

Tobback, E., Decostere, A., Hermans, K., Haesebrouck, F., Chiers, K., 2007. *Yersinia ruckeri* infections in salmonid fish. J. Fish Dis. 30, 257–268.

Toranzo, A.E., Hetrick, F.M., 1982. Comparative stability of two salmonid viruses and poliovirus in fresh, estuarine and marine waters. J. Fish dis. 5, 223–231.

Wallace, I.S., Gregory, A., Murray, A.G., Munro, E.S., Raynard, R.S., 2008. Distribution of infectious pancreatic necrosis virus (IPNV) in wild marine fish from Scottish waters with respect to clinically infected aquaculture sites producing Atlantic salmon, *Salmo salar* L. J. Fish Dis. 31, 177–186.

Willumsen, B., 1989. Birds and wild fish as potential vectors of *Yersinia ruckeri*. J. Fish Dis. 12, 275–277.

Webb, C.R., 2005. Farm animal networks: unraveling the contact structure of the British sheep population. Prev. Vet. Med. 68, 3–17.